Negative-Ion Electron Capture Dissociation of MALDI-Generated Peptide Anions

Steven A. DeFiglia, Carson W. Szot, Kristina Håkansson*

Department of Chemistry, University of Michigan, Ann Arbor, MI 48109-1055, United States

*Corresponding author.

Email: kicki@umich.edu

Phone: +1-734-615-0570

Abstract: Negative ion electron capture dissociation (niECD) is an anion MS/MS technique that provides fragmentation analogous to conventional ECD, including high peptide sequence coverage and retention of labile posttranslational modifications (PTMs). niECD has been proposed to be most efficient for salt-bridged, zwitterionic precursor ion structures. Several important PTMs, e.g., sulfation and phosphorylation, are acidic and can therefore be challenging to characterize in positive ion mode. Furthermore, PTM-friendly techniques such as ECD require multiple precursor ion positive charges. By contrast, singly-charged ions, refractory to ECD, are most compatible with niECD. Because electrospray ionization typically yields multiply-charged ions, we sought to explore matrix assisted laser desorption/ionization (MALDI) in combination with niECD. However, the requirement for zwitterionic gaseous structures may preclude efficient niECD of MALDI-generated anions. Unexpectedly, we found that niECD of anions from MALDI is not only possible, but proceeds with similar or higher efficiency compared with ESI-generated anions. Matrix selection does not appear to have a major effect. With MALDI, niECD is demonstrated up to m/z ~4300. For such larger analytes, multiple electron captures are observed, resulting in triply-charged fragments from singly-charged precursor ions. Such charge-increased fragments show improved detectability. Furthermore, significantly improved (~20-fold signal-to-noise increase) niECD spectral quality is achieved with equivalent sample amounts from MALDI vs. ESI. Overall, the reported combination with MALDI significantly boosts the analytical utility of niECD.

Introduction:

Bottom-up proteomics is a well-established area for protein identification and site determination of posttranslational modifications (PTMs).[1,2] This approach typically involves digestion of proteins into peptides and their analysis with positive ion mode (nano)electrospray ionization (ESI)-tandem mass spectrometry (MS/MS).[1] While much less common, negative ion mode analysis can provide complementary peptide identifications and improved ionization as well as stability of acidic PTMs such as phosphorylation and sulfation.[3] These common PTMs perform various biological roles, e.g., facilitating protein-protein interactions,[4–7] but can be difficult to characterize with conventional positive ion mode MS/MS activation methods.[8] Specifically vibrationally activating methods like collision induced dissociation and infrared multiphoton dissociation may yield high sequence coverage but often cause preferential ejection or migration of labile PTMs.[9–12]

Electron capture dissociation (ECD)[13] and electron transfer dissociation (ETD)[14] can retain PTMs but require multiply charged cations which exacerbates the challenge of acidic PTM characterization.[15] Electron induced dissociation (EInD) in which singly charged cations[16] or anions[17] are irradiated with ≥8 eV electrons have also shown partial PTM retention; however, the resulting spectra are complex with multiple fragment ion types and abundant neutral losses. Negative mode ETD[18] and electron detachment dissociation (EDD)[19] can retain labile modifications but are most effective at high charge states/low m/z ratios,[20] yield abundant, structurally uninformative neutral losses, and show overall low fragmentation efficiency. Negative ion mode free radical initiated peptide sequencing (nFRIPS)[15] and ultraviolet photodissociation (UVPD)[21] have been demonstrated to retain the highly labile sulfate PTM but both techniques, similar to EInD, yield complex MS/MS spectra that can be difficult to annotate. In addition, nFRIPS involves multiple stages of chemical derivatization/clean-up and benefits from an MS^3 implementation, not available on all mass spectrometers.

Negative ion ECD[22] (niECD) involves electron capture by peptide anions to yield charge-increased radical species that dissociate into predominately PTM-retaining $c'/z^{\bullet}$-type fragments from backbone N-C_α bond cleavage, analogous to conventional ECD/ETD. We have recently shown that salt-bridged, zwitterionic gaseous peptide anion structures with, e.g., one protonated and two deprotonated sites for an overall singly charged anion, undergo efficient niECD.[23] We further proposed that electron capture occurs at or near the positively-charged site,[22,23] similar to

conventional cation ECD/ETD.[24,25] This mechanism was examined in detail by subjecting five sets of peptides with decreasing probability of forming gaseous zwitterions to niECD.[23] These experiments showed that a lower zwitterion probability correlated with decreased niECD efficiency and sequence coverage. Furthermore, niECD was effective for sulfated cholecystokinin (CCKS, DyMGWMDF) but not for its desulfated form (CCK).[22] However, low efficiency niECD of CCK was enabled by chemical derivatization that increases the likelihood of zwitterion formation.[23] Liquid/solid-phase amino acid zwitterions[26–30] are well recognized; however, the concept is still controversial in the gas phase.[28,29] Nevertheless, experimental and theoretical evidence for gas phase salt-bridged zwitterionic structures has been presented for, e.g., ESI-generated arginine as well as larger peptides.[31–34] In addition to the zwitterion requirement, electrons must overcome a Coulomb barrier to enable capture by anions. Consequently, slightly higher energy (~2.5-7 eV) electrons than in conventional ECD (≤1 eV) are optimal[22,35] and niECD is most efficient for singly charged anions. Such low charge states can be difficult to generate at high abundance with ESI, particularly for larger peptides.

In contrast to ESI, matrix-assisted laser desorption/ionization (MALDI) primarily generates singly charged ions under typical conditions.[36] Thus, MALDI is mostly incompatible with ECD, ETD, and EDD; however MALDI-ECD has been demonstrated at higher ion source pressure at which multiply charged precursor ions can be generated.[37] *c*- and *z*-type fragments from in-source decay were once attributed to ECD events within the plume, but hydrogen/deuterium exchange experiments have since supported a hydrogen atom driven mechanism.[38–40] Though heavily studied in positive ion mode, there is still disagreement about the MALDI mechanism with cluster, photoionization, and autoprotolysis theories all having merit.[41–47] In the cluster model, preformed ions are moved from the solid- to the gas phase in matrix clusters, luckily surviving neutralization events in the post-ablation plume.[38] In photoionization models matrix excitation yields $M^{+\bullet}$ (in which M is the neutral analyte), or low energy electrons released from the metal target plate are captured by the matrix forming $M^{-\bullet}$. In both these scenarios, hydrogen abstraction to or from the analyte must occur to result in protonated/deprotonated analyte ions. In autoprotolysis, 2M spontaneously becomes (de)protonated due to heating, forming $[M + H]^+$ and $[M - H]^-$. Following the initial ionization step, secondary proton transfer processes between the matrix and the analyte occur prior to matrix-analyte cluster breakup.[42,48] In positive ion mode, Jaskolla and Karas observed that the ratio of lucky survivor (cluster) ions to gas phase proton

transfer ions increased as functions of analyte size, reduced laser fluence, and solvent acidity.[43] Critically, their unified mechanism excludes deprotonated lucky survivor ions from acidic matrices due to the higher gas-phase amide backbone basicity compared with the acidic matrix.[49–51] This argument does not account for salt bridge stabilization which, in the gas phase, severely reduces peptide basicity.[52] However, if a net-neutral peptide with a salt bridge is moved to the gas phase and then undergoes deprotonation, the conditions for niECD would be fulfilled. Also, MALDI-generated zwitterions were previously reported for net-neutral zwitterionic pH indicator dyes in positive ion mode and for fixed positive charge glyco-phosphocholines in negative ion mode.[53,54]

Here, we demonstrate that MALDI-niECD is not only feasible but can be superior to ESI-niECD for a variety of peptides with and without PTMs and other chemical modifications. We examine several MALDI matrices and expand the m/z range of niECD. Experiments are also presented to evaluate the niECD zwitterion mechanism in the context of MALDI.

Materials and Methods:

Materials

Hirudin and cholecystokinin sulfopeptides were purchased from BACHEM (Torrence, CA). β-casein phosphopeptide was acquired from Anaspec (Fremont, CA), human peptide YY was sourced from resbio (Natick, MA). Synthetic peptides were purchased from GenicBio (Shanghai, China) or Genscript (Piscatawy, NJ). Acetic anhydride (99%), 2,5-dihydroxybenzoic acid (DHB), sinapinic acid (SA), 4-chloro-cyanocinnamic acid (Cl-CCA), 9-aminoacridine (9AA), 1,5-diaminonaphthalene (DAN), N,N,N′,N′-tetramethyl-1,8-naphthalenediamine (proton sponge, PS), α-cyano-4-hydroxycinnamic acid (CHCA), insulin chain B, pardaxin, and bovine ubiquitin were purchased from Sigma-Aldrich. Nanospheres (2.2 nm diameter) were purchased from Nanopartz™ (Loveland, CO). Optima LC-MS-grade water, methanol (MeOH), isopropanol (IPA), acetonitrile (ACN), neat trifluoroacetic acid (TFA), and triethylamine (TEA), were purchased from Fisher scientific.

Sample Preparation

Analyte-matrix mixtures were prepared in either 70:30 H_2O/ACN with of 0.1% TFA (TA30) or 25:75 IPA/MeOH at 1:10 v/v ratio. For SA, saturated matrix in ethanol was spotted prior to

spotting the analyte in the double layer approach. Hirudin and CCKS were N-terminally acetylated in 25:75 acetic anhydride/methanol.[55] Acetylated peptides were vacuufuged, reconstituted in 100 μL H_2O, combined with CHCA, and spotted onto the MALDI target plate using the dried droplet method.

Mass Spectrometry

All experiments were performed on a 7 T quadrupole-Fourier transform ion cyclotron resonance (Q-FT-ICR) mass spectrometer (Bruker Daltonics, Billerica, MA). This instrument is equipped with a Paracell detector,[56] a hollow cathode electron source,[57] a 1 kHz smartbeam II frequency-tripled 355 nm Nd:YAG laser, and a MTP 384 ground steel MALDI target plate.

ESI-generated net singly deprotonated hirudin was used to optimize niECD prior to MALDI experiments. Random smart walk at medium laser focus with ~24% power and 200 laser shots per scan were used for all MALDI experiments. MALDI-niECD was performed with - (5-7) V cathode bias and - (4-6) V lens voltage at 1.5-1.6 A current for up to 10 seconds. The Paracell trapping electrodes were set to – 1.5 V in all experiments with the exception of analytes larger than m/z 2,200, for which – 3 V were used.

Data Analysis

MS/MS fragment ion annotations were performed manually using Bruker Compass DataAnalysis, version 5.0 SR1. ProteinProspector (https://prospector.ucsf.edu/prospector/mshome.htm) was used for calculation of theoretical monoisotopic m/z values. Peptide sequence coverage was displayed with an in-house python script.

Results and Discussion:

niECD of MALDI- vs ESI-Generated Net Singly Deprotonated Hirudin

Our previous work has shown that the sulfopeptide hirudin undergoes highly efficient niECD.[20] The most abundant niECD fragment ion from net singly charged, $[M - H]^-$, hirudin is a double neutral loss ($NH_3 + CO_2$) at m/z 714.3 (2-) from the charge-increased species, $[M - H]^{2-\bullet}$, formed upon electron capture. This fragment is excellent for tuning as it provides evidence for electron capture due to the increased charge. By contrast, the $[M - H]^{2-\bullet}$ species overlaps with the artifactual second harmonic of the precursor ion and, thus, niECD efficiency can be difficult to assess based

on the latter signal. niECD of MALDI-generated net singly charged hirudin anions is shown in **Figure 1**. Despite substantial sulfonate loss observed in the MS^1 spectrum (data not shown), MALDI resulted in nearly 20-fold signal increase for the sulfated 714.3 tuning fragment

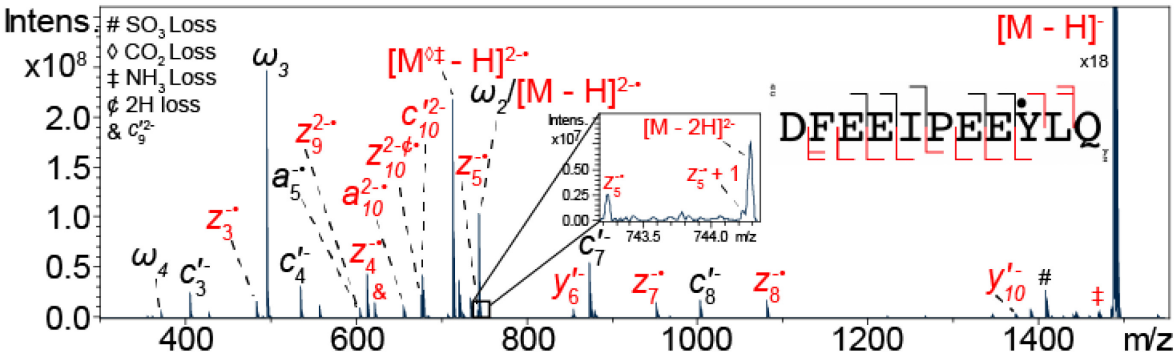

Figure 1. Hirudin MALDI-niECD MS/MS spectrum. niECD was performed with – 5 V cathode bias, 3 s irradiation, 16 scans. 1 µL peptide at 10 µM was spotted on the MALDI plate. ● = sulfotyrosine. Fragments in red retain sulfation.

compared with ESI when using the same amount of material to prepare the MALDI plate as was consumed during ESI (Supplementary Figure 1). Only a fraction of the material on the MALDI plate was consumed during data acquisition. Overall, the niECD spectra from MALDI- vs. ESI-generated hirudin are quite similar, including 100% sulfate retention in sequence-informative fragment ions. However, the improved signal-to-noise ratio in MALDI-niECD allowed for detection of the low abundance z_5• fragment, not previously observed with ESI-niECD (64 scans, 5 s irradiation)[20], with 16 scans, 3 s irradiation (Fig. 1 inset) for 100% sequence coverage. Furthermore, sequence coverage from a single scan at 1 s irradiation showed the same sequence coverage as previous ESI-niECD (Supplementary Figure 2). The c_6' fragment, complementary to z_5• overlaps with the isotopic distribution of the $[M - H]^{2-\bullet}$/second harmonic and is thus obscured in the spectrum. Similar to ESI-niECD, MALDI-niECD results in several doubly charged c'/z•-type fragment ions from the singly charged precursor anion.

We also compared the electron energy regimes for ESI-niECD vs. MALDI-niECD. As shown in Supplementary Figure 3, nearly identical electron energy requirements were observed, peaking at a ~- 5 V cathode bias. MALDI niECD fragmentation efficiency and sequence coverage are similar independent of matrix chemical structure and pKa (**Figure 2** and Supplementary Figure 4). The latter observation was surprising as matrices with high or low pKas were unexpected to produce zwitterionic analytes as different dominating ionization mechanisms would be expected to alter the ratio of zwitterions/non zwitterions in the sample. This result may be due to the acidity

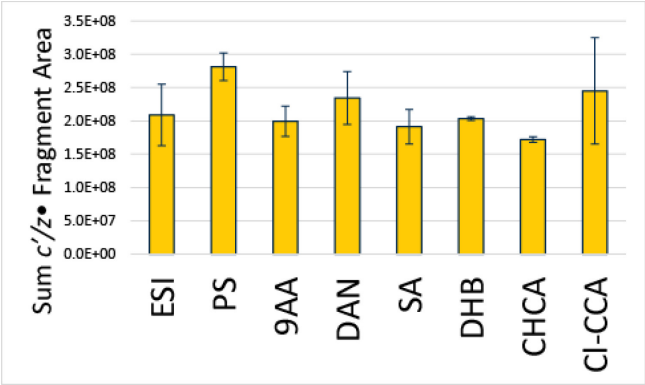

Figure 2. Summed abundance of *c′/z•* fragments from niECD of hirudin following ESI vs MALDI with various matrices. Precursor ion abundance was ~8x10^8 in all experiments

of hirudin, which contains seven acidic sites and only one basic site. Thus, a zwitterionic structure is favored. In addition, the intermediate pressure MALDI source on the SolariX instrument may alleviate analyte ion internal energy differences resulting from different matrices. Two nanometer diameter gold nanospheres, likely operating through a different ionization mechanism[58] than the matrices shown in Figure S4, were also implemented but yielded lower precursor ion signal and required higher laser power (50% rather than ~24%; Supplementary Figure 5). Unfortunately this higher laser power resulted in near-total precursor ion desulfation for both polyvinylpyrrolidone- and citrate-capped nanoparticles. On the other hand, signature niECD charge increased fragments were observed for desulfated hirudin, suggesting the presence of gaseous zwitterions.

Peptide Primary Structure Effects in MALDI- vs. ESI-niECD

Our previous work showed that compact salt-bridged, presumably zwitterionic, precursor ion structures are required for efficient niECD of electrosprayed analytes.[23] While there is evidence for overall cationic zwitterions from ESI,[31,59,60] less is known about net anionic zwitterions. By contrast, gaseous zwitterions are not typically associated with MALDI although some work has been reported with zwitterionic dyes.[53] We performed MALDI-niECD on a set of six hirudin-derived synthetic peptides (P1-P6) with decreasing acidity, achieved by replacing acidic amino acids with more neutral ones (**Figure 3, right**). These peptides were previously examined by ESI-niECD on a different instrument.[23] We directly compared ESI-niECD to MALDI-niECD on a newer instrument with the same niECD parameters, as shown in **Figure 3, left**. Fragmentation efficiency in MALDI-niECD decreases with decreasing peptide acidity, similar to ESI-niECD although the trends are not identical. However, more acidic peptides, more likely to have zwitterionic structures, show the highest niECD efficiency in both ESI and MALDI. These data from both ESI and MALDI-niECD are also comparable to our previous ESI-niECD results.[23]

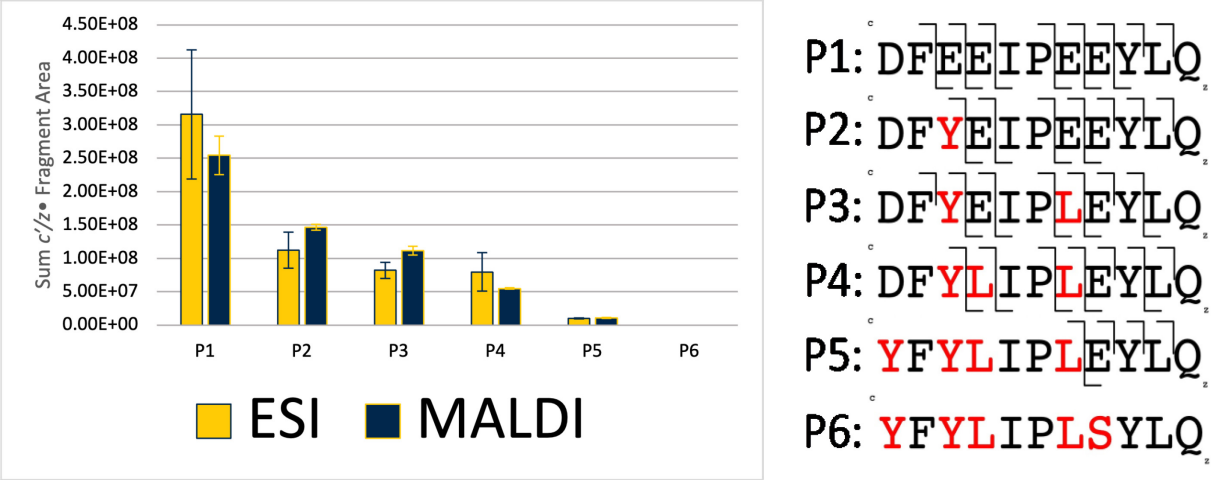

Figure 3. Left: Sum of $c'/z\bullet$ fragments at ~3x10^8 precursor ion abundance for a set of synthetic peptides, P1-P6 (Left). Sequence coverage based on $c'/z\bullet$ fragments for peptides P1-P6 (Right). 1 µL peptide at 100 µM in saturated CHCA was spotted on the MALDI plate.

Another strategy for affecting the probability of a gas-phase zwitterionic peptide structure is to chemically derivatize basic[22] or acidic[23] sites to more neutral sites for decreased zwitterion propensity. The only basic site in hirudin, the N-terminal amine, was acetylated and the resulting derivatized peptide was subjected to MALDI-niECD (Supplementary Figure 6, bottom). Compared with underivatized hirudin under the same conditions (Figure S6, top), only a moderate fragment abundance decrease is observed for some fragment ions, e.g., c'_4^- and c'_7^-. On the other hand, some other fragments, e.g., c'_{10}^{2-}, y'_8^- and $z_9^{-\bullet}$, increase in abundance. One explanation may be that the N-acetylated N-terminus or the slightly basic proline residue still allow a zwitterionic structure. While such protonation may be less likely in most peptides, hirudin is highly acidic with six carboxylic acids, i.e., a zwitterionic structure seems likely for an overall singly deprotonated species. Alternatively, conventional positive ion mode ECD has been shown to be sensitive to peptide gas-phase structure.[61] Thus, these observations may indicate similar effects in niECD. However, because hirudin shows highly efficient niECD, acetylation may be expected to only have a moderate effect in contrast to another sulfopeptide, CCKS (with two acidic sites), which was previously shown to yield significantly lower ESI-niECD efficiency upon acetylation.[22] We subjected acetylated CCKS to MALDI-niECD and observed a similar effect (Supplementary Figure 7). Overall, these results suggest that MALDI-generated net singly charged anions have similar structures compared with ESI-generated anions and that salt-bridged structures are favored in both ESI-[23] and MALDI-niECD.

MALDI-niECD at Extended Mass Range

While niECD can fragment multiply-charged anions,[22] this MS/MS technique is most efficient for singly charged anions due to decreased Coulomb repulsion between anions and electrons. Because MALDI preferentially yields singly-charged analyte ions, even at higher mass, the ability to couple niECD with MALDI also enabled experiments with larger peptides. A singly phosphorylated β-casein tryptic peptide was previously subjected to niECD in its net doubly deprotonated form following ESI.[22] While good sequence coverage was observed, long irradiation time (20 s) was required. We compared ESI-niECD of the same doubly net deprotonated peptide with MALDI-niECD of the net singly deprotonated peptide with irradiation for 5 s (Supplementary Figure 8). These data were acquired for different numbers of scans to ensure that the remaining precursor ion ($[M - 2H]^{2-}$ vs. $[M - H]^{-}$) had the same abundance. Similar to previous ESI-niECD,[22] a slightly higher electron energy was required for the net doubly deprotonated species (- 8 vs. - 7 V cathode bias). Under these conditions, MALDI-niECD was significantly more efficient, resulting in 100%

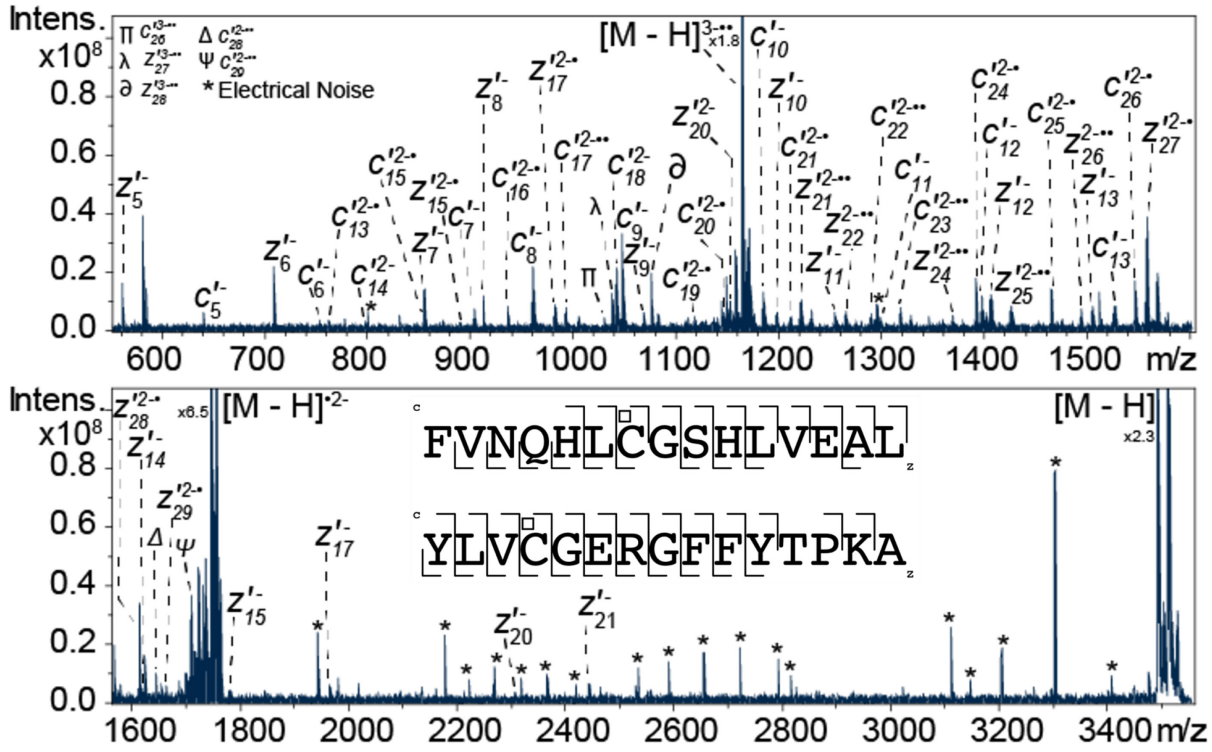

Figure 4. MALDI-niECD MS/MS spectrum of oxidized insulin, chain B. Lower m/z region (Top) and higher m/z region (Bottom). niECD was performed with – 7 V cathode bias, 10 s irradiation, 64 scans. Saturated SA (0.5 μL) followed by 0.5 μL peptide at 100 μM was spotted using the double layer method. □ = oxidized cysteine.

sequence coverage with observation of nearly all possible *c′* and *z*•-type fragment ions, including 100% phosphate retention (Supplementary Figure 8, top). Sequence coverage from ESI-niECD was lower than previously observed, presumably due to the shorter irradiation time. Also, for multiply-charged precursor anions, competition between electron capture and detachment occurs, further lowering niECD efficiency. While electron detachment is typically optimum ~19 eV,[62] electrons can be turned around by the ion transfer optics, which has previously been discussed in so called "multipass" ECD.[63,64] While singly-charged precursor ions (m/z 2059) are observed in ESI, their low abundance prohibits effective niECD.

With this exciting result for the β-casein phosphopeptide, we attempted MALDI-niECD of even larger peptides. MALDI-niECD of net singly deprotonated pardaxin (m/z 3320) is shown in Supplementary Figure 9. At 10 s irradiation, - 7 V bias voltage, and 64 scans, a high S/N ratio spectrum was obtained with high sequence coverage, only missing two potential *c′/z*• fragments. Singly-, doubly- and triply-charged fragment ions are observed from the singly charged precursor ion. Note that single and double electron capture results in hypervalent species one and two hydrogen atoms heavier than the corresponding doubly and triply deprotonated species in which each charge corresponds to a deprotonated site rather than an added electron, e.g., a difference of one hydrogen atom. However, for larger peptides, hydrogen migration to form *z′* rather than *z*•-type ions, also corresponding to a difference of one hydrogen atom, is relatively common, thus we

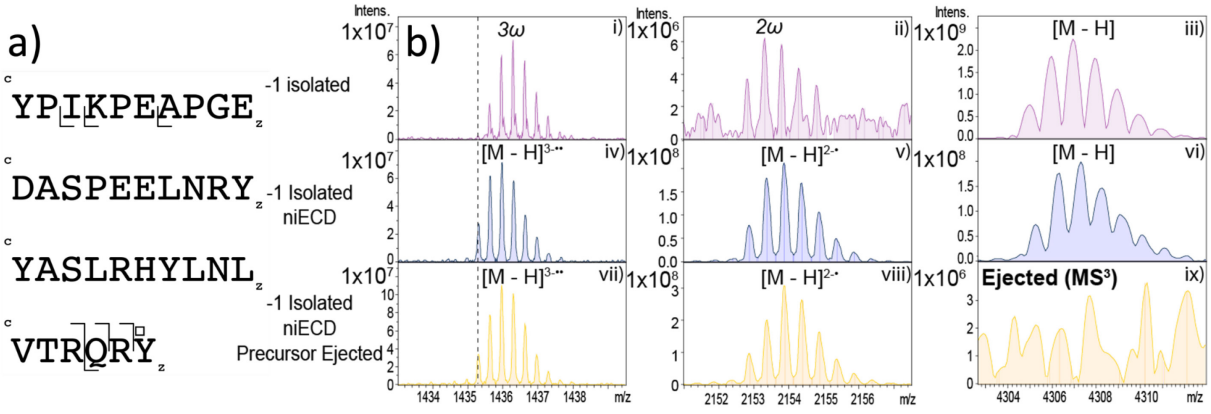

Figure 5. niECD of net singly deprotonated peptide YY. a) Sequence coverage. b) Zoomed in regions of the precursor ion (iii, vi, and ix), second harmonic region (ii, v, and viii), and third harmonic region (i, iv, vii) following quadrupole-isolation only (i-iii), electron irradiation (iv-vi), and electron irradiation + precursor ion ejection (vii-ix). Both single (v, viii) and double (iv, vii) electron capture was observed upon electron irradiation. Saturated SA (0.5 μL) followed by 0.5 μL peptide at 125 μM was spotted using the double layer method. □ = amidation.

cannot differentiate between these ion types. Due to the high charge density in these experiments, some peak splitting, resulting in degraded mass accuracy was noted, particularly at high m/z ratio. For net singly deprotonated insulin chain B (m/z 3495), even higher quality data were obtained with MALDI-niECD, showing fragmentation at all possible N-Cα backbone bonds, as shown in **Figure 4**. Similar to the pardaxin MALDI-niECD, singly-, doubly, and triply-charged fragments were observed. The even larger peptide YY (m/z 4307) showed more limited fragmentation (**Figure 5a** and Supplementary Figure 10). However, highly efficient single and double electron capture to yield $[M - H]^{2-\bullet}$ and $[M - H]^{3-\bullet\bullet}$ charge-increased species was observed. Note that the latter species may not be biradicals; however, this notation is common for keeping track of electron charge carriers.[65] For the isolated, but not irradiated, net singly charged precursor ion (**Figure 5b**, iii)), a relatively low abundance second harmonic (Fig. 5b, ii) and a relatively abundant third harmonic (Fig. 5b, i) are present. Upon irradiation, significant generation of the $[M - H]^{2-\bullet}$ charge-increased species (Fig. 5b, v) is noted on top of the second harmonic as the abundance of this signal increases by >20-fold while the $[M - H]^-$ precursor ion (Fig. 5b, vi) decreased ~10-fold. No significant signal increase is seen for the third harmonic (Fig. 5b, iv); however, hydrogen atom ejection is observed, highlighted by the dotted line. To further verify the origin of these signals, the precursor ion was selectively ejected from the ICR cell via a CHEF excitation sweep (Fig. 5b, ix). The abundances of the annotated $[M - H]^{2-\bullet}$ and $[M - H]^{3-\bullet\bullet}$ species were not affected (Fig. 5b vii and viii), ascertaining that these are not artifactual signals. Double electron capture had not previously been observed in ESI-niECD. Such outcomes imply that MALDI not only can generate zwitterions, but zwitterions with multiple positively and negatively charged sites.

A final attempt at increasing niECD mass range involved electron irradiation of net singly deprotonated ubiquitin (m/z ~8600). Surprisingly, a shorter irradiation time (0.5 s) was more effective at producing a charge increased species at ~4281 m/z compared with the 10 s used for optimum MALDI-niECD of pardaxin, insulin chain B, and peptide YY (Supplementary Figure 11). Because ubiquitin is significantly larger than the aforementioned peptides, the charge density increase upon electron capture is lower, possibly contributing to this process being more favorable. As seen in Fig. S11 (Right), the precursor ion signal is mostly depleted upon electron irradiation, supporting the $[M - H]^{2-\bullet}$ product assignment. Also, no second harmonic artifactual signal was observed in the absence of electron irradiation (Fig. S11, Left). While observation of the $[M - H]^{2-\bullet}$ species is exciting, no fragment ions were observed, likely due to the low precursor ion signal.

This low signal is not surprising due to the basic nature of ubiquitin and the expected poor ion transmission to the ICR cell at this m/z ratio.

Conclusions:

The presented data demonstrate that niECD of MALDI-generated anions is not only possible but superior to niECD of ESI-generated anions. MALDI typically generates singly charged ions, which are most compatible with niECD due to decreased Coulomb repulsion. We showed that niECD of MALDI-generated singly charged anions allows for nearly 20-fold greater signal compared with ESI-niECD with equivalent material. Unexpectedly, niECD efficiency was not observed to be matrix dependent, indicating generation of similar peptide gas-phase structures independent of matrix pKa. Peptide derivatization to promote or reduce the probability of a net negatively-charged zwitterionic state correlated with niECD efficiency, similar to ESI-generated anions. MALDI allowed niECD at m/z values >~2,000 (the previously observed limit with ESI) with high sequence coverage up to m/z ~3,500 and limited sequence coverage up to m/z ~4,300. Furthermore, we observed intriguing multiple electron capture, resulting in both doubly- and triply-charged fragments from singly-charged precursor anions. Overall, these results present a strategy for improving the analytical utility of niECD.

ASSOCIATED CONTENT

Supporting Information:

The following supporting information is available free of charge at ACS website http://pubs.acs.org (Figure S1) Hirudin ESI-niECD vs. MALDI-niECD at fixed sample amount; (Figure S2) Hirudin MALDI niECD, single scan; (Figure S3) Electron energy regimes for ESI-niECD and MALDI-niECD at fixed precursor ion abundance; (Figure S4) Hirudin ESI-niECD vs. MALDI-niECD with a variety of matrices; (Figure S5); SALDI niECD of desulfated hirudin; (Figure S6) Quantification of niECD fragments from hirudin vs. N-acetylated hirudin; (Figure S7) Quantification of niECD fragments from CCKS vs. N-Acetylated CCKS; (Figure S8) β-casein phosphopeptide niECD efficiency for the 1- and 2- charge states; (Figure S9) niECD of pardaxin; (Figure S10) Peptide YY niECD; (Figure S11) Electron capture by ubiquitin anions

Acknowledgements: This work was supported by National Science Foundation grant CHE2004043. S.A.D was partially supported by a George Ashworth Summer Fellowship. Scott Daniels is acknowledged for invaluable support of the FT-ICR instrument. The Paracell was acquired through an equipment supplement to NIH grant R01GM139916.

References:

(1) Zhang, Y.; Fonslow, B. R.; Shan, B.; Baek, M. C.; Yates, J. R. Protein Analysis by Shotgun/Bottom-up Proteomics. *Chem. Rev.* **2013**, *113*, 2343–2394.

(2) Miller, R. M.; Smith, L. M. Overview and Considerations in Bottom-up Proteomics. *Analyst* **2022**, *148*, 475–486.

(3) Bigwarfe, P. M.; Wood, T. D. Effect of Ionization Mode in the Analysis of Proteolytic Protein Digests. *Int. J. Mass Spectrom.* **2004**, *234*, 185–202.

(4) Ardito, F.; Giuliani, M.; Perrone, D.; Troiano, G.; Muzio, L. Lo. The Crucial Role of Protein Phosphorylation in Cell Signaling and Its Use as Targeted Therapy. *Int. J. Mol. Med.* **2017**, *40*, 271–280.

(5) Farzan, M.; Mirzabekov, T.; Kolchinsky, P.; Wyatt, R.; Cayabyab, M.; Gerard, N. P.; Gerard, C.; Sodroski, J.; Choe, H. Tyrosine Sulfation of the Amino Terminus of CCR5 Facilitates HIV-1 Entry. *Cell* **1999**, *96*, 667–676.

(6) Borghei, A.; Ouyang, Y.-B.; Westmuckett, A. D.; Marcello, M. R.; Landel, C. P.; Evans, J. P.; Moore, K. L. Targeted Disruption of Tyrosylprotein Sulfotransferase-2, an Enzyme That Catalyzes Post-Translational Protein Tyrosine O-Sulfation, Causes Male Infertility*. *J. Biol. Chem.* **2006**, *281*, 9423–9431.

(7) Westmuckett, A. D.; Hoffhines, A. J.; Borghei, A.; Moore, K. L. Early Post-Natal Pulmonary Failure and Primary Hypothyroidism in Mice with Combined TPST-1 and TPST-2 Deficiency. *Gen. Comp. Endocrinol.* **2008**, *156*, 145–153.

(8) Kweon, H. K.; Kong, A. T.; Hersberger, K. E.; Huang, S.; Nesvizhskii, A. I.; Wang, Y.; Hakansson, K.; Andrews, P. C. Sulfoproteomics Workflow with Precursor Ion Accurate Mass Shift Analysis Reveals Novel Tyrosine Sulfoproteins in the Golgi. *J. Proteome Res.* **2024**, *23*, 71–83.

(9) Palumbo, A. M.; Smith, S. A.; Kalcic, C. L.; Dantus, M.; Stemmer, P. M.; Reid, G. E. Tandem Mass Spectrometry Strategies for Phosphoproteome Analysis. *Mass Spectrom. Rev.* **2011**, *30*, 600–625.

(10) Håkansson, K.; Chalmers, M. J.; Quinn, J. P.; McFarland, M. A.; Hendrickson, C. L.; Marshall, A. G. Combined Electron Capture and Infrared Multiphoton Dissociation for Multistage MS/MS in a Fourier Transform Ion Cyclotron Resonance Mass Spectrometer. *Anal. Chem.* **2003**, *75*, 3256–3262.

(11) Adamson, J. T.; Håkansson, K. Infrared Multiphoton Dissociation and Electron Capture Dissociation of High-Mannose Type Glycopeptides. *J. Proteome Res.* **2006**, *5*, 493–501.

(12) Little, D. P.; Speir, J. P.; Senko, M. W.; O'Connor P.B; Mclafferty, F. W. Infrared Multiphoton Dissociation of Large Multiply Charged Ions for Biomolecule Sequencing. *Rapid Commun. Mass Spectrom.* **1994**, *66*, 1403–1406.

(13) Zubarev, R. A.; Kelleher, N. L.; McLafferty, F. W. Electron Capture Dissociation of Multiply Charged Protein Cations. A Nonergodic Process. *J. Am. Soc. Mass Spectrom.* **1998**, *120*, 3265–3266.
(14) Syka, J. E. P; Coon, J. J.; Schroeder, M. J.; Shabanowitz, J.; Hunt, D. F. Peptide and Protein Sequence Analysis by Elecron Transfer Dissociation Mass Spectrometry. *Proc. Natl. Acad. Sci. U.S.A*. **2004**, *101*, 9528-9533.
(15) Borotto, N. B.; Ileka, K. M.; Tom, C. A. T. M. B.; Martin, B. R.; Håkansson, K. Free Radical Initiated Peptide Sequencing for Direct Site Localization of Sulfation and Phosphorylation with Negative Ion Mode Mass Spectrometry. *Anal. Chem.* **2018**, *90*, 9682–9686.
(16) Baba, T.; Rajabi, K.; Liu, S.; Ryumin, P.; Zhang, Z.; Pohl, K.; Causon, J.; LeBlanc, J. C.; Y.; Kurogochi, M. Electron Impact Excittation of Ions from Organics on Singly Protonated Peptides with and without Post-Translational Modifications. *J. Am. Soc. Mass Spectrom*. **2022**, *33*, 1723−1732.
(17) Kalli, A.; Grigorean, G.; Hakansson, K. Electron Induced Dissociation of Singly Deprotonated Peptides. *J. Am. Soc. Mass Spectrom*. **2011**, *22*, 2209-2221.
(18) Coon, J. J.; Shabanowitz, J.; Hunt, D. F.; Syka, J. E. P. Electron Transfer Dissociation of Peptide Anions. *J. Am. Soc. Mass Spectrom.* **2005**, *16*, 880–882.

(19) Budnik, B. A.; Haselmann, K. F.; Zubarev, R. A. Electron Detachment Dissociation of Peptide Di-Anions: An Electron-Hole Recombination Phenomenon. *Chem. Phys. Lett.* **2001**, *342*, 299–302.
(20) Hersberger, K. E.; Håkansson, K. Characterization of O-Sulfopeptides by Negative Ion Mode Tandem Mass Spectrometry: Superior Performance of Negative Ion Electron Capture Dissociation. *Anal. Chem.* **2012**, *84*, 6370–6377.
(21) Robinson, M. R.; Moore, K. L.; Brodbelt, J. S. Direct Identification of Tyrosine Sulfation by Using Ultraviolet Photodissociation Mass Spectrometry. *J. Am. Soc. Mass Spectrom.* **2014**, *25*, 1461–1471.
(22) Yoo, H. J.; Wang, N.; Zhuang, S.; Song, H.; Håkansson, K. Negative-Ion Electron Capture Dissociation: Radical-Driven Fragmentation of Charge-Increased Gaseous Peptide Anions. *J. Am. Chem. Soc.* **2011**, *133*, 16790–16793.
(23) Wang, N.; Dixit, S. M.; Lee, T.; DeFiglia, S. A.; Ruotolo, B. T.; Hakansson, K. Salt-Bridged Peptide Anion Gaseous Structures Enable Negative Ion Electron Capture Dissociation. *J. Am. Soc. Mass Spectrom.* **2024**, *accepted*.
(24) Simons, J. Mechanisms for S-S and N-Cα Bond Cleavage in Peptide ECD and ETD Mass Spectrometry. *Chem. Phys. Lett.* **2010**, *484*, 81–95.
(25) Syrstad, E. A.; Tureček, F. Toward a General Mechanism of Electron Capture Dissociation. *J. Am. Soc. Mass Spectrom.* **2005**, *16*, 208–224.
(26) Borsook, H.; Macfadyen, D. A. The Effect of Isoelectric Amino Acids on the PH of a Phosphate Buffer Solution a Contribution in Support of the "Zwitter Ion Hypothesis." *J. Gen. Physiol.* **1930**, *13*, 509–527.
(27) Cohn, E. J. Contrasting Properties of Ions, Zwitterions and Uncharged Molecules. *Science* **1934**, *79*, 83–84.
(28) Locke, M. J.; Hunter, R. L.; Melver, R. T. Jr. Experimental Determination of the Acidity and Basicity of Glycine in the Gas Phase. *J. Am. Chem. Soc.* **1979**, *101*, 272-273.
(29) Jensen, J. H.; Gordon, M. S. On the Number of Water Molecules Necessary To Stabilize the Glycine Zwitterion. *J. Am. Chem. Soc* **1995**, *117*, 8159–8170.

(30) Bjerrum, N. Die Konstitution Der Ampholyte, Besonders Der Aminosäuren, Nnd Ihre Dissoziationskonstanten. *Z. Physik. Chem.* **1923**, *104*, 147–173.
(31) Price, W. D.; Jockusch, R. A.; Williams, E. R. Is Arginine a Zwitterion in the Gas Phase? *J. Am. Chem. Soc.* **1997**, *119*, 11988–11989.
(32) Julian, R. R.; Jarrold, M. F. Gas-Phase Zwitterions in the Absence of a Net Charge. *J. Phys. Chem. A* **2004**, *108*, 10861–10864.
(33) Schnier, P. D.; Price, W. D.; Jockusch, R. A.; Williams, E. R. Blackbody Infrared Radiative Dissociation of Bradykinin and Its Analogues: Energetics, Dynamics, and Evidence for Salt-Bridge Structures in the Gas Phase. *J. Am. Chem. Soc.* **1996**, *118*, 7178–7189.
(34) Bonner, J.; Lyon, Y. A.; Nellessen, C.; Julian, R. R. Photoelectron Transfer Dissociation Reveals Surprising Favorability of Zwitterionic States in Large Gaseous Peptides and Proteins. *J. Am. Chem. Soc.* **2017**, *139*, 10286–10293.
(35) Kjeldsen, F.; Haselmann, K. F.; Budnik, B. A.; Jensen, F.; Zubarev, R. A. Dissociative Capture of Hot (3-13 EV) Electrons by Polypeptide Polycations: An Efficient Process Accompanied by Secondary Fragmentation. *Chem. Phys. Lett.* **2001**, *356*, 201–206.
(36) Knochenmuss, R.; Zenobi, R. MALDI Ionization: The Role of in-Plume Processes. *Chem. Rev.* **2003**, *103*, 441–452.
(37) Frankevich, V.; Zhang, J.; Dashtiev, M.; Zenobi, R. Production and Fragmentation of Multiply Charged Ions in "Electron-Free" Matrix-Assisted Laser Desorption/Ionization. *Rapid Commun. Mass Spectrom.* **2003**, *17*, 2343–2348.
(38) Karas, M.; Glückmann, M.; Schäfer, J. Ionization in Matrix-Assisted Laser Desorption/Ionization: Singly Charged Molecular Ions Are the Lucky Survivors. *J. Mass Spectrom.* **2000**, *35*, 1–12.
(39) Köcher, T.; Engström, Å.; Zubarev, R. A. Fragmentation of Peptides in MALDI In-Source Decay Mediated by Hydrogen Radicals. *Anal. Chem.* **2005**, *77*, 172–177.
(40) Takayama, M. N-Cα Bond Cleavage of the Peptide Backbone via Hydrogen Abstraction. *J. Am. Soc. Mass Spectrom.* **2001**, *12*, 1044–1049.
(41) Bae, Y. J.; Kim, M. S. A Thermal Mechanism of Ion Formation in MALDI. *Annu. Rev. Anal. Chem.* **2015**, *8*, 41–60.
(42) Knochenmuss, R. Ion Formation Mechanisms in UV-MALDI. *Analyst* **2006**, *131*, 966–986.
(43) Jaskolla, T. W.; Karas, M. Compelling Evidence for Lucky Survivor and Gas Phase Protonation: The Unified MALDI Analyte Protonation Mechanism. *J. Am. Soc. Mass Spectrom.* **2011**, *22*, 976–988.
(44) Karas, M.; Krüger, R. Ion Formation in MALDI: The Cluster Ionization Mechanism. *Chem. Rev.* **2003**, *103*, 427–439.
(45) Zenobi, R.; Knochenmuss, R. Ion Formation in MALDI Mass Spectrometry. *Mass Spectrom. Rev.* **1998**, *17*, 337–366.
(46) Knochenmuss, R. A Quantitative Model of Ultraviolet Matrix-Assisted Laser Desorption/Ionization. *J. Mass Spectrom.* **2002**, *37*, 867–877.
(47) Setz, P. D.; Knochenmuss, R. Exciton Mobility and Trapping in a MALDI Matrix. *J. Phys. Chem. A* **2005**, *109*, 4030–4037.
(48) Ehring, H.; Karas, M.; Hillenkamp, F. Role of Photoionization and Photochemistry in Ionization Processes of Organic Molecules and Relevance for Matrix-assisted Laser Desorption Lonization Mass Spectrometry. *Org. Mass Spectrom.* **1992**, *27*, 472–480.
(49) O'Hair, R. A. J.; Bowieb, J. H.; Gronertb, S. Gas Phase Acidities of the α Amino Acids*. *Int. J Mass Spectrom. Ion Processes* **1992**, *111*, 23–36.

(50) Mirza, S. P.; Raju, N. P.; Vairamani, M. Estimation of the Proton Affinity Values of Fifteen Matrix-Assisted Laser Desorption/Ionization Matrices under Electrospray Ionization Conditions Using the Kinetic Method. *J. Am. Soc. Mass Spectrom.* **2004**, *15*, 431–435.
(51) Li, Z.; Matus, M. H.; Velazquez, H. A.; Dixon, D. A.; Cassady, C. J. Gas-Phase Acidities of Aspartic Acid, Glutamic Acid, and Their Amino Acid Amides. *Int. J. Mass Spectrom.* **2007**, *265*, 213–223.
(52) Marchese, R.; Grandori, R.; Carloni, P.; Raugei, S. On the Zwitterionic Nature of Gas-Phase Peptides and Protein Ions. *PLoS Comput. Biol.* **2010**, *6*, 1–11.
(53) Krüger, R.; Pfenninger, A.; Fournier, I.; Glückmann, M.; Karas, M. Analyte Incorporation and Ionization in Matrix-Assisted Laser Desorption/Ionization Visualized by PH Indicator Molecular Probes. *Anal. Chem.* **2001**, *73*, 5812–5821.
(54) Stanton, R.; Hykollari, A.; Eckmair, B.; Malzl, D.; Dragosits, M.; Palmberger, D.; Wang, P.; Wilson, I. B. H.; Paschinger, K. The Underestimated N-Glycomes of Lepidopteran Species. *Biochim. Biophys. Acta* **2017**, *1861*, 699–714.
(55) Lindh, I.; Sjövall, J.; Bergman, T.; Griffiths, W. J. Negative-Ion Electrospray Tandem Mass Spectrometry of Peptides Derivatized with 4-Aminonaphthalenesulphonic Acid. *J. Mass Spectrom.* **1998**, *33*, 988–993.
(56) Boldin, I. A.; Nikolaev, E. N. Fourier Transform Ion Cyclotron Resonance Cell with Dynamic Harmonization of the Electric Field in t. *Rapid Commun. Mass Spectrom.* **2011**, *25*, 122–126.
(57) Tsybin, Y. O.; Witt, M.; Baykut, G.; Kjeldsen, F.; Håkansson, P. Combined Infrared Multiphoton Dissociation and Electron Capture Dissociation with a Hollow Electron Beam in Fourier Transform Ion Cyclotron Resonance Mass Spectrometry. *Rapid Commun. Mass Spectrom.* **2003**, *17*, 1759–1768.
(58) Song, K.; Cheng, Q. Desorption and Ionization Mechanisms and Signal Enhancement in Surface Assisted Laser Desorption Ionization Mass Spectrometry (SALDI-MS). *Appl. Spectrosc. Rev* **2020**, *55*, 220–242.
(59) Bush, M. F.; O'Brien, J. T.; Prell, J. S.; Saykally, R. J.; Williams, E. R. Infrared Spectroscopy of Cationized Arginine in the Gas Phase: Direct Evidence for the Transition from Nonzwitterionic to Zwitterionic Structure. *J. Am. Chem. Soc.* **2007**, *129*, 1612–1622.
(60) Freitas, M. A.; Marshall, A. G. Rate and Extent of Gas-Phase Hydrogen/Deuterium Exchange of Bradykinins: Evidence for Peptide Zwitterions in the Gas Phase. *Int. J. Mass Spectrom.* **1999**, *182/183*, 221–231.
(61) Mihalca, R.; Kleinnijenhuis, A. J.; McDonnell, L. A.; Heck, A. J. R.; Heeren, R. M. A. Electron Capture Dissociation at Low Temperatures Reveals Selective Dissociations. *J. Am. Soc. Mass Spectrom.* **2004**, *15*, 1869–1873.
(62) Yang, J.; Mo, J.; Adamson, J. T.; Hakansson, K. Characterization of Oligodeoxynucleotides by Electron Detachment Dissociation Fourier Transform Ion Cyclotron Resonance Mass Spectrometry. *Anal. Chem*. **2005**, *77*, 1876-1882.
(63) McFarland, M. M.; Chalmers, M. J.; Quinn, J. P.; Hendrickson, C. L.; Marshall, A. G. Evaluation and Optimization of Electron Capture Dissociation Efficiency in Fourier Transform Ion Cyclotron Resonance Mass Spectrometry. *J. Am. Soc. Mass Spectrom*. **2005**, *16*, 1060-1066.
(64) Tsybin, Y. O.; Quinn, J. P.; Tsybin, O. Y.; Hendrickson, C. L.; Marshall, A. G. Electron Capture Dissociation Implementation Progress in Fourier Transform Ion Cyclotron Resonance Mass Spectrometry. *J. Am. Soc. Mass Spectrom*. **2008**, *19*, 762-771.

(65) Kleinnijenhuis, A, J.; Heck, A. J. R.; Duursma, M. C.; Heeren, R. M. A. Does Double Electron Capture Lead to the Formation of Biradicals? An ECD-SORI-CID Study on Lacticin 481. *J. Am. Soc. Mass Spectrom*. **2005**, *16*, 1595-1601.

For TOC Only: